

# An experimental investigation of the stress-rupture behaviour of a parallel-lay aramid rope

J. J. CHAMBERS\*, C. J. BURGOYNE‡

*Department of Civil Engineering, Imperial College of Science and Technology, London SW7 2BU, UK*

The results from a series of short-term stress-rupture tests on a parallel-lay aramid rope are presented. General trends of behaviour are established from lifetime and strain data; the results provide a firm basis around which methods of predicting long-term stress-rupture response may be developed.

## 1. Introduction

The durability of concrete as a structural material has received a great deal of recent attention owing to a growing number of problems; the major concern with structural concrete is the susceptibility of steel reinforcement or steel tendons to corrosion. A new material, which does not corrode, and which may offer a suitable alternative to steel, has been developed by ICI Linear Composites Ltd. The material, known as Parafil Type G<sup>§</sup>, is a synthetic rope consisting of continuous parallel yarns of the aramid fibre Kevlar 49<sup>¶</sup>.

Tests have shown that Parafil ropes have adequate strength and stiffness for use as prestressing tendons [1, 2]; tensile strengths in excess of  $1925 \text{ N mm}^{-2}$  are consistently measured while the Young's modulus of the material is typically around  $118 \text{ kN mm}^{-2}$ . Parafil Type G ropes of 6 tonnes and 60 tonnes nominal breaking load (NBL) are shown in Fig. 1. The nominal breaking load is calculated on the conservative assumption that the ultimate stress is  $1925 \text{ N mm}^{-2}$  [3].

Although ultimate strength and modulus of elasticity are the most important short-term properties of any structural material, they provide little information about its behaviour when subjected to permanent loads. When some materials are exposed to stresses less than their initial ultimate stress for long periods of time, they eventually creep to failure. Hence, when determining suitable operating stresses for these materials questions of "lifetime under stress", and creep deformation are more pertinent.

The operating conditions of prestressing tendons present a particularly extreme example since, for structural reasons, tendons need to be permanently highly stressed. Indeed, steel tendons, which are permanently stressed to 70% of their ultimate strength, are the most heavily loaded members known to the authors. A deep understanding of the time-dependent

nature of stress-rupture in Parafil ropes is clearly required therefore, if full advantage is to be taken of their high inherent strength. Without this understanding it would be necessary to apply large factors of safety to the short-term strength of Parafil which would make it a less viable alternative when compared with more traditional materials. For instance, while the initial strength of Parafil exceeds that of steel tendons, the latter do not exhibit a stress-rupture phenomenon at ambient temperature (except when subject to stress-corrosion). The long-term behaviour of Parafil ropes, at high stress levels is, therefore, of fundamental significance to their application in prestressed concrete.

This paper presents the results from a series of constant load stress-rupture tests on 60 tonne Type G Parafil ropes. This size of ropes was chosen for study since they are the smallest ropes manufactured that would be used as prestressing tendons in practical applications. Furthermore, owing to the large number of yarns in a 60 tonne rope and the statistical properties of large bundles [1] it is probable that when consideration is given to other Parafil ropes of a size suitable for application in the field of prestressing, the effects of rope size may be effectively ignored.

Stress-rupture data for most materials tends to be well scattered and so ideally an extensive testing programme involving hundreds of specimens ought to have been undertaken to give a full understanding. However, from the moderate number of tests conducted here, it will be shown that it is possible to establish overall trends of stress-rupture behaviour on the basis of both lifetime and strain measurements. Having established these trends, advantage will be taken later [4] of the various existing theoretical and practical approaches to stress-rupture in polymers to predict more reliably the long-term stress-rupture behaviour of Parafil ropes.

\* *Present Address:* Central Electricity Generating Board, London Headquarters, UK.

‡ *Present Address:* Cambridge University Engineering Department, Trumpington St, Cambridge, CB2 1PZ, UK.

§ *Trademark of ICI Linear Composites Ltd., UK.*

¶ *Trademark of E.I. Du Pont de Nemours.*

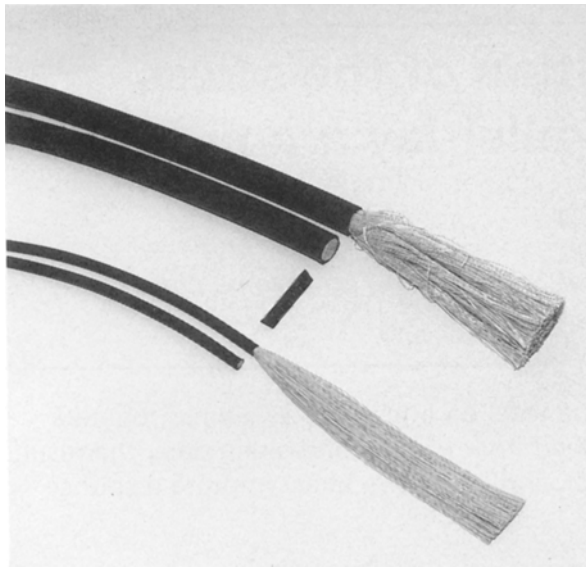


Figure 1 6 tonne and 60 tonne Parafil ropes.

## 2. Test procedure and instrumentation

All the ropes were tested within a steel box-section which acted as a stiff and structurally efficient reaction-frame. The box-section of 8 m length had been shown in short-term tension tests [1] to be sufficiently long to eliminate rope end-effects. Loads were applied to the ropes through a pull-rod located in the centre-hole of a hydraulic jack and connected to the rear end of a modified rope terminal. A diagram of the stressing arrangement is shown in Fig. 2

Parafil ropes are supplied on circular drums. Therefore, prior to applying the creep load, all ropes were pretensioned (to 60% of the nominal breaking load) in order to remove any minor disorientation of the fibre lay caused by the coiling process. The creep loads themselves were applied using the load-maintaining facility of a hydraulic machine; an automatic "cut-out" device enabled tests to be left running unattended.

Creep loads were measured using four electrical

resistance foil-type strain gauges glued to the steel box-section. A linear variable displacement transformer, monitored with a data acquisition system, was used to measure creep displacements.

## 3. Test results

Sixteen stress-rupture tests at stresses ranging from 68 to 95% of the nominal breaking stress, and with failure times extending to five months, were performed. General results are shown in Table I.

### 3.1. Times to break

Stress-rupture lifetime data is commonly plotted using stress against  $\log(\text{lifetime})$  coordinates since this choice often leads to a linear plot and hence facilitates extrapolation of the results. Fig. 3 shows the Parafil results plotted in this manner and although a considerable degree of scatter is observed in the rope lifetimes (as expected), a linear trend between applied stress and the logarithm of the "time to break" may be interpreted.

### 3.2. Creep strains

Figs 4 to 7 illustrate the creep behaviour of the ropes; generally, an initial region of high creep rate was displayed (primary creep) followed by an almost linear steady-state secondary creep region. The onset of failure was usually characterized by a dramatic rise in the creep rate which coincided with an increase in the frequency with which yarns within the rope could be heard to fail. The amount of creep strain associated with the sudden upturn in the creep curve (tertiary creep) prior to failure was found to be arbitrary and usually occurred over a small timescale. In some cases the sudden upturn was not discernible; on other occasions it was not observed owing to the policy of taking strain readings at fixed time intervals. Of greater engineering value than the somewhat arbitrary final creep strain, however, is the magnitude of the strain marking the end of secondary creep and hence, the onset of failure; the dependence of this strain ( $\epsilon_s$ ) on the creep load is shown in Fig. 8.

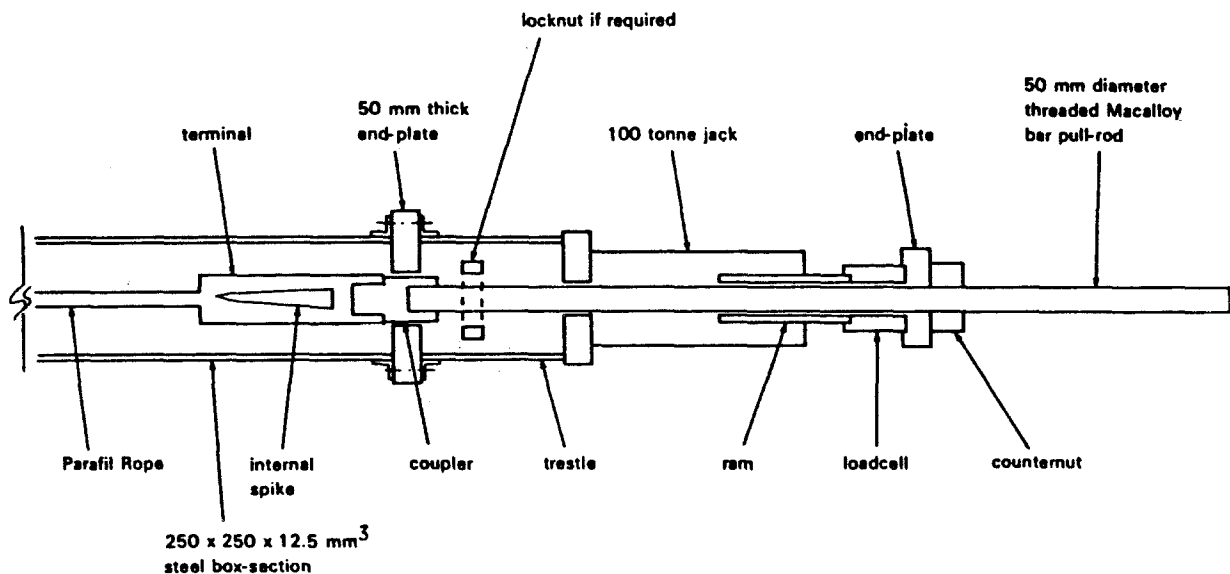


Figure 2 Laboratory stressing system for 60 tonne ropes.

TABLE I Stress relaxation test results.

Test No.	Applied load (kN)	% NBL	Time to break ( $t_b$ )			$\log_{10}(t_b)$ (min)	Strain at 1 min $\epsilon_1$ (%)	Extrapolated final strain $\epsilon_f$ (%)	Final creep strain $\epsilon_f - \epsilon_1$ (%)
			days	h	min				
1	531	90	-	2	15	2.130	1.569	1.656	0.087
2	560	95	immediate			-	1.640	1.640	0
3	501	85	-	-	27	1.431	1.519	1.573	0.054
4	469	79.5	-	2	0	2.079	1.407	1.480	0.073
5	459	78	-	3	31	2.324	failed inside terminal		-
6	449	71*	11	22	57	4.236	1.232	*	-
7	503	85.5	-	22	35	3.132	1.519	1.635	0.116
8	507	86	-	2	41	2.207	1.519	1.598	0.079
9	532	90.5	-	1	3	1.799	1.649	1.727	0.078
10	548	93	-	-	10	1.000	1.674	1.714	0.040
11	441	75	-	4	25	2.423	failed next to terminal		-
12	470	80	-	18	56	3.055	1.418	1.481	0.063
13	441	75	11	3	55	4.206	1.323	1.401	0.078
14	411	70	power failure			-	-	-	-
15	456	77.5	-	17	10	3.013	1.362	1.426	0.064
16†	412	68	155	3	42	5.349	†	1.326	-

\*conducted at two load levels – first load quoted; final strain not relevant

†subject to intermittent overstress of 4% NBL during first 2 h –  $\epsilon_1$  inaccurate

Test 6 was subjected to a load of 71% NBL (for which the mean  $t_b$  from Equation 1 is 39600 min) for 81.77% of the total time, and 81% NBL (for which the mean  $t_b$  is 1196 min) for the remaining 18.23% of the time. On the assumption that damage accumulates as a proportion of the “time to break” spent at each load level, then the equivalent load ( $p$ ) can be found from

$$\frac{0.8177}{39600} + \frac{0.1823}{1196} = \frac{1}{a \log(15.39 - 15.2p)}$$

which leads to an equivalent load of 76.5% NBL. This value has been used to plot the result of this test on the figures, but has not been taken into account in the derivation of Equation 1.

When creep strains are plotted against the logarithm of time a linear dependence is quickly established (Fig. 9). The dependence does not remain linear, however, and in all tests the rate of creep (with log time) was found to increase as failure was approached. The initial strains recorded upon reaching the required stress level were found to be greater (by an average of 6%) than those expected on the basis of the average modulus observed in short-term tension tests [1]. The increase was almost certainly due to the much slower loading rate associated with the load-maintaining facility of the hydraulic cabinet. The increased strains are also consistent with the observed high primary creep rates.

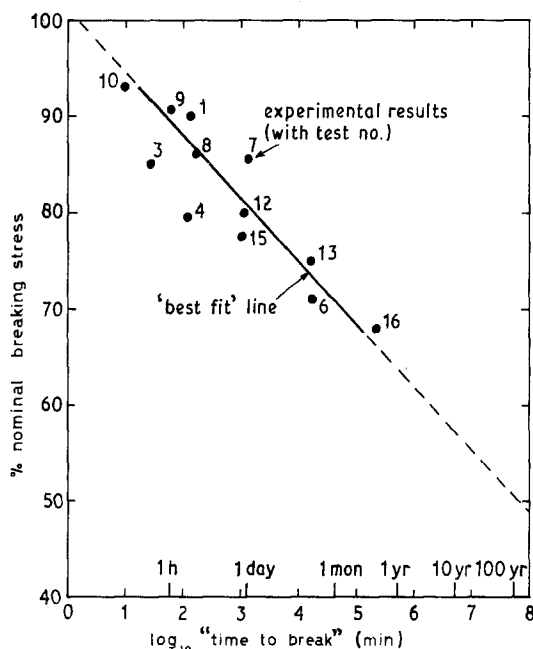


Figure 3 Stress rupture test results.

#### 4. Empirical predictions of long-term stress rupture

##### 4.1 Based on “times to break”

A “best-fit” line for the experimental values of “time to break” could be extrapolated to enable predictions of lifetimes at lower stress levels to be made (Fig. 3). A linear relationship between stress and the logarithm of lifetime is consistent with various reaction rate theories for stress-rupture [4]. Hence, there is considerable theoretical justification for the extrapolation of this line. The equation for the “best-fit” line, determined using the method of least squares, is found to be

$$\log_{10} t_b = 15.39 - 15.2f \tag{1}$$

$$0.68 \leq f \leq 0.93$$

where  $f$  is the static stress as a proportion of nominal breaking load and  $t_b$  the time to break (min). The result from Test 2 (at 95% nominal breaking load (NBL)) in which the rope failed immediately upon reaching the required load and which would be classed as an outlier in Fig. 3, has not been included in the derivation of Equation 1. Similarly, Test 6 has been ignored, since it was carried out at two load levels, and so have the tests which failed within the termination. At high stress levels, with low “times to break”, the time spent at intermediate stress levels during the loading process will lead to failure times which are not consistent with results obtained at lower stress levels (where the time spent on the loading phase is insignificant by comparison with the total duration of the test).

A typical structural design life for prestressed concrete members is 100 years. The extrapolated “best-fit” line for the experimental lifetime data (Fig. 3)

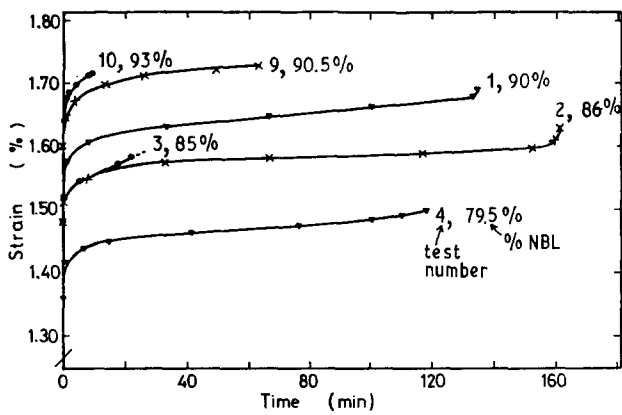


Figure 4 Creep strain curves for tests 1, 2, 3, 4, 9 and 10.

indicates that a load equal to 50% of the nominal breaking load would cause creep failure after this time period.

#### 4.2. Based on strain

The measurement of creep strains during the stress-rupture tests was initially considered to be less important than the recording of "times to break" since lifetime data enables predictions of rope lifetimes (outside the stress range investigated) to be made directly. However, as the test programme progressed, certain trends began to emerge between the measured creep strains and the magnitude of the applied stress, which provided the motivation for considering a method for making lifetime predictions (at stresses lower than those considered on the test programme) based on creep strain data. For the predictions based on strain data to have any credibility the method would, at the very least, have to yield good agreement with the experimentally observed stress-rupture lifetimes.

Three trends were observed in the stress-rupture tests:

- (1) The magnitude of the creep strain marking the end of the secondary creep phase and the onset of rope failure increased with the applied stress.
- (2) The strain at the end of the loading phase (i.e. the strain at the beginning of primary creep) increased as the applied stress increased (in accordance with the broadly linear stress-strain curve for Parafil).
- (3) The rate of creep strain increased with stress.

Mathematical representations of these trends may be combined to enable alternative lifetime predictions for Parafil Type G ropes to be made.

##### 4.2.1. Secondary creep strains

Fig. 8 shows the dependence of the creep strain,  $\epsilon_s$ ,

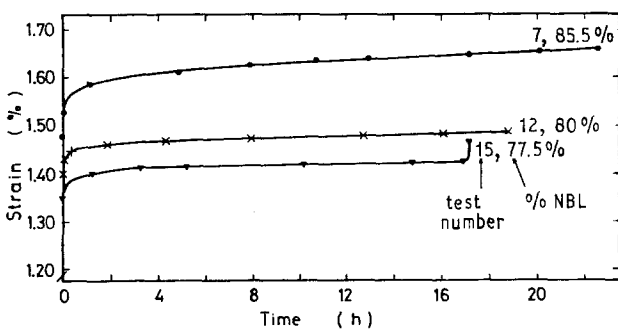


Figure 5 Creep strain curves for tests 7, 12 and 15.

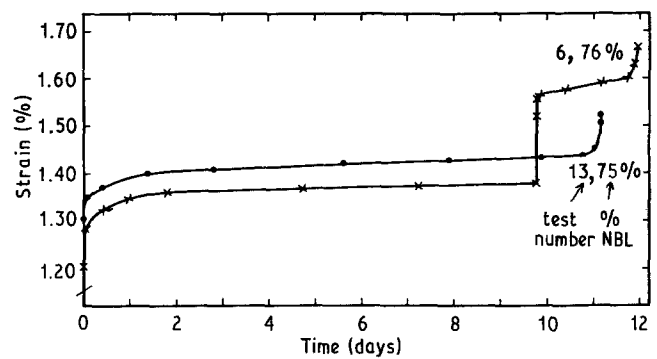


Figure 6 Creep strain curves for tests 6 and 13.

measured at the end of the secondary creep phase, on the applied stress. It can be inferred that the onset of creep failure is dependent on a limiting strain which increases linearly with stress.

Similarly, if the predominantly linear plots of strain against log-time (Fig. 9) are assumed to remain totally linear until failure occurs, i.e. any upward sweep in the creep curve is ignored, then an alternative limiting or failure strain,  $\epsilon_f$ , may be defined. The dependence of the strain  $\epsilon_f$  on the applied stress is also linear as illustrated in Fig. 10; moreover, since the strain  $\epsilon_f$  is extracted from plots of strain against log time (as opposed to absolute time) it is more suited to inclusion in the creep-strain method for lifetime predictions.

When a linear regression analysis is performed on the data for the limiting strain  $\epsilon_f$  and the corresponding values of applied stress (Fig. 10) a correlation coefficient of 0.98 is obtained. The equation of the "best-fit" line is found to be

$$\epsilon_f = 1.736f + 0.111$$

$$0.68 \leq f \leq 0.93 \quad (2)$$

##### 4.2.2. Initial strains

Since Parafil Type G ropes display broadly linear stress-strain behaviour, a linear relationship between the strain measured at the end of the loading phase (i.e. at the start of primary creep) and the applied stress would be expected. For mathematical convenience, however, the strain ( $\epsilon_i$ ) measured one minute after reaching the required stress level is taken as the initial strain; nevertheless, the linearity still

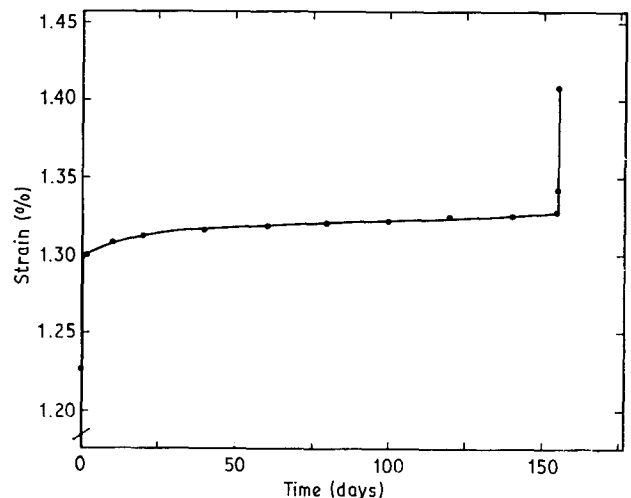


Figure 7 Creep strain curves for test 16.

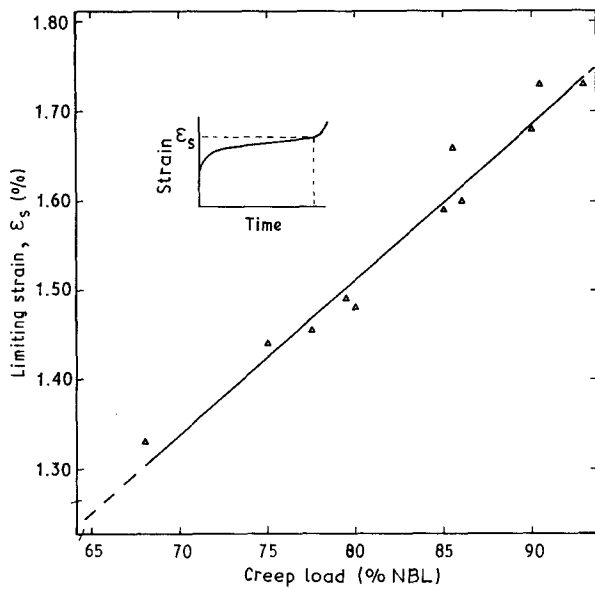


Figure 8 Strain at end of secondary creep plotted against load.

holds as shown in Fig. 11. The equation representing the “best fit” line for this data is found to be

$$\begin{aligned} \varepsilon_i &= 1.951 f - 0.147 \\ 0.71 &\leq f \leq 0.93 \end{aligned} \quad (3)$$

Owing to a problem of maintaining a constant load during the first two hours of Test 16 the observed initial strain for this test was not included in the regression analysis. The coefficient of correlation for the remaining data was found to be 0.99; hence, Equation 3 represents the experimental data well.

#### 4.2.3. Creep strain capacity

Having obtained expressions for the limiting strain  $\varepsilon_f$  (Equation 2) and the initial strain (Equation 3) the dependence on the applied stress of the creep strain capacity or the amount of creep that a rope is able to undergo before it ruptures ( $\varepsilon_f - \varepsilon_i$ ) may be expressed as

$$\begin{aligned} (\varepsilon_f - \varepsilon_i) &= 0.258 - 0.215 f \\ 0.71 &\leq f \leq 0.93 \end{aligned} \quad (4)$$

Fig. 12 indicates that the capacity for undergoing

creep strain before failure increases as the applied stress decreases.

#### 4.2.4. Creep rates as a function of logarithmic time

The creep strain capacity increases gradually as the applied stress decreases (Fig. 12); this observation is only compatible with the expectation of much increased lifetimes at lower stresses if the rate of creep reduces significantly with stress. Fig. 13 indicates that the rate of creep does indeed diminish rapidly as the applied static stress is reduced. Here, the creep rate is taken as the gradient of the linear portion of the creep strain against log time plots (Fig. 9); this rate is consistent with the notion of an extrapolated limiting strain  $\varepsilon_f$ .

To enable rational lifetime predictions to be made a power curve of the form  $y = ax^b$  has been fitted to the creep rate data (using a standard curve fitting computer program); power curves of this form pass through the origin so this choice seems realistic. The approximate relationship between the creep rate and the applied stress is given by

$$\begin{aligned} r &= 0.060 f^{3.52} \\ 0.68 &\leq f \leq 0.93 \end{aligned} \quad (5)$$

Experimental values for the creep rate and the “best-fit” power curve are shown in Fig. 13.

#### 4.2.5. Lifetime predictions

Stress-rupture lifetime predictions for Parafil Type G ropes based on experimentally recorded strain data may now be derived from a combination of the relationships defining the dependence of the creep strain capacity and the rate of creep on the applied stress (Equations 4 and 5). Based on the observed rope behaviour and the assumptions made, the following equation is appropriate for predicting lifetimes

$$\log_{10} t_b = \frac{(\varepsilon_f - \varepsilon_i)}{r} \quad (6a)$$

$$= 4.3 f^{-3.52} - 3.58 f^{-2.52} \quad (6b)$$

where  $r$  is the creep rate (% strain per decade. A

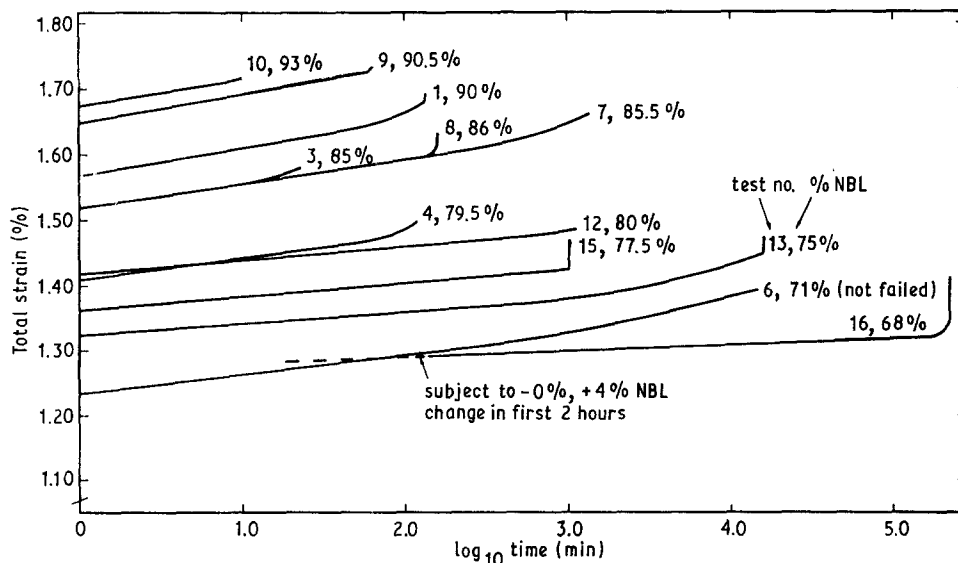


Figure 9 Creep strains plotted against logarithmic time.

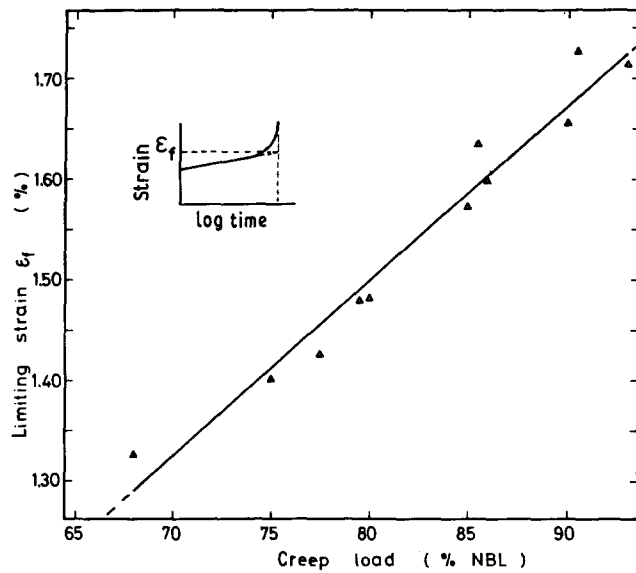


Figure 10 Limiting strain (projected to failure time) plotted against load.

decade is one increment on a  $\log_{10}$  scale). Fig. 14 illustrates the results of applying Equation 6 and provides a comparison with the experimental lifetime data. The lifetime predictions based on the strain criteria are in good agreement with the experimental lifetime data over the range of stress investigated. When stresses outside the test range are considered, however, the two extrapolations shown in Fig. 14 diverge, with the creep-strain method leading to predictions of much longer lifetimes at lower stresses than the direct extrapolation of the experimental lifetime results. The loads estimated to produce a creep failure after 100 years from a consideration of strains and from a consideration of lifetime data are 67% NBL and 50% NBL respectively.

#### 4.2.6. Creep rates from lifetime data

It is possible, using Equation 6a, to generate creep rate data which correspond to the experimental lifetime results. This can be achieved by substituting the equation representing the "best-fit" line of the lifetime data (Equation 1) and the assumed creep strain

capacity (Equation 4) into Equation 6a and solving for the rate parameter  $r$ , which yields

$$r = \frac{0.258 - 0.215f}{15.39 - 15.2f} \quad (7)$$

The results of following this procedure are also shown in Fig. 13. There is reasonable agreement between the "generated" creep rate data and the experimentally recorded data over the range of stress investigated. This implies that the correlation between applied stress and creep strain capacity (Equation 4) is not simply fortuitous. Outside the investigated stress range however, (i.e. at lower stresses) the "generated" creep rate curve diverges significantly from the experimental power law curve, levelling-off at around 0.018% creep strain per decade. The divergence is largely coincident with the divergence of the two alternative lifetime curves shown in Fig. 14.

Predictions of stress-rupture lifetimes at low stresses

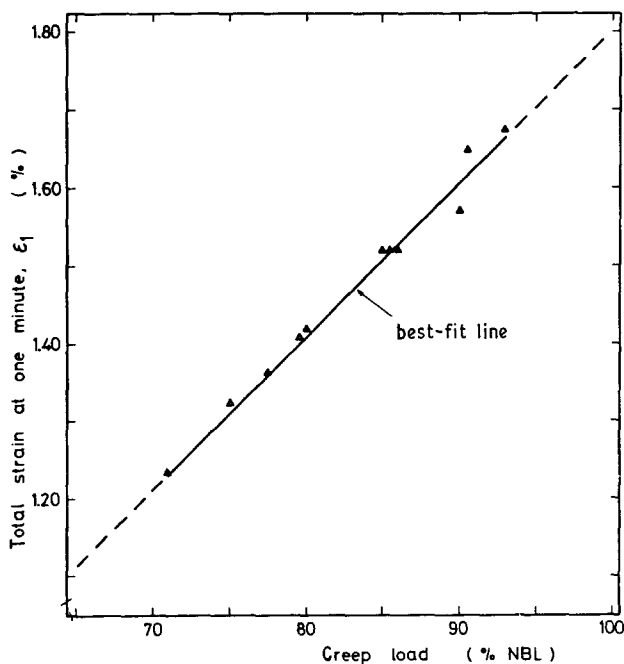


Figure 11 Strain at one minute plotted against load.

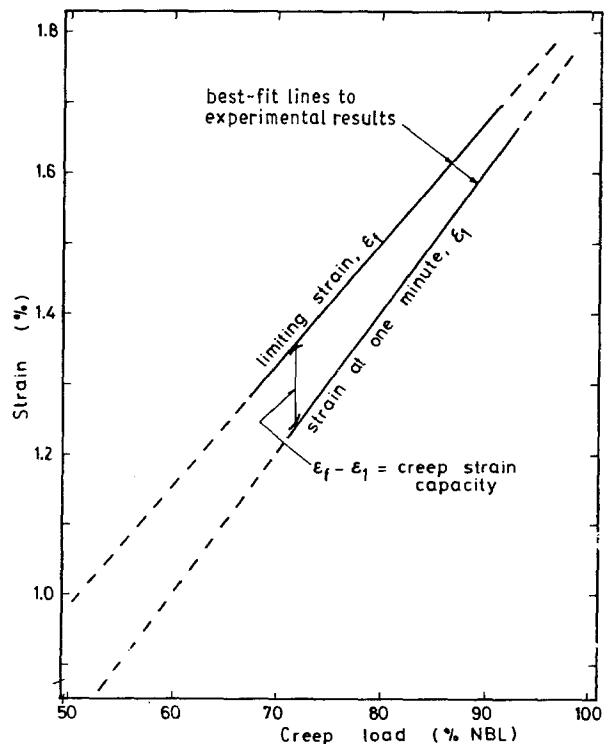


Figure 12 Creep strain capacity plotted against load.

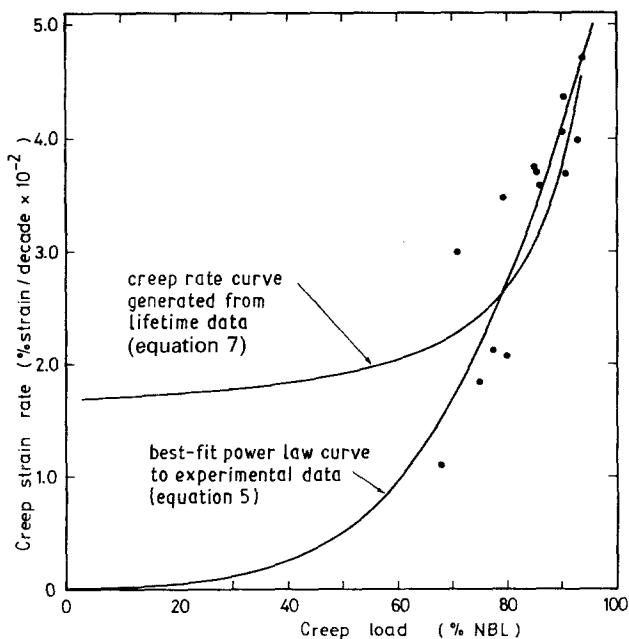


Figure 13 Creep strain rates plotted against load.

(based on strain criteria) are clearly very much dependent on the assumed correlation between creep rate and stress. If tests were conducted to measure creep rates at low stresses and the results agreed with the power law curve of Fig. 13 then lifetime predictions based on strain criteria (i.e. curve 2 of Fig. 14) would be favoured. If experimental creep rates at low stress levels were found to agree with the “generated” creep rate curve of Fig. 13, however, this would strongly favour an extrapolation of the “best-fit” line to the experimental lifetime data (i.e. curve 1 of Fig. 14).

Strong theoretical justification exists for extrapolation of the “best-fit” line to the experimental lifetime data [4]. Also, a value for the creep strain rate of Kevlar 49 yarns and fibres, applicable to a wide range of low working stresses, which is often quoted in the literature [5, 6] is 0.02% per decade. This gives good agreement with the “generated” creep rate curve which, at low stresses, levels-off at about 0.018% strain per decade.

Strong arguments exist in favour of extrapolating the experimental lifetime data but further tests to measure the creep strain rate of Parafil at low stresses

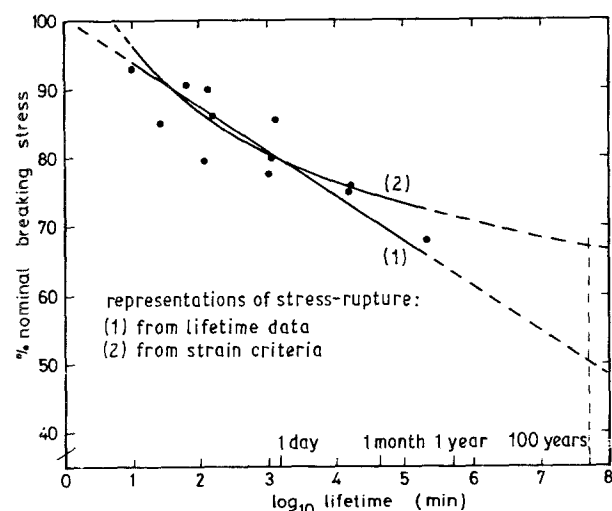


Figure 14 Predicted “time to break” plotted against load.

are required. Such tests are currently underway at Imperial College and elsewhere and the results will be reported in due course.

## 5. Appraisal of empirical long-term stress-rupture predictions

The method of predicting long-term stress-rupture lifetimes, based on strain measurements taken during a series of relatively short-term tests, should be used guardedly. For instance, the notion of a creep-strain capacity which increases only marginally as the applied stress is reduced, is purely empirical and cannot be supported theoretically. Also, lifetime predictions for Parafil at typical operating stresses (using this method) are very dependent on the assumed creep rate. In general, the creep rates quoted for Kevlar 49 fibres at the lower end of the stress scale, exceed those for Parafil determined from the power law (Equation 5). There are, therefore, doubts as to the validity of the assumed power law to describe creep rates for Parafil outside the investigated stress range and so for the time being stress-rupture predictions for Parafil based on strain measurements should be considered as optimistic.

A linear extrapolation of the “best-fit” line for the lifetime data, on the other hand, seems well justified. A straight line not only fits the data reasonably well but is consistent with reaction rate theories for creep [4]. Furthermore, a linear dependence of the logarithm of the lifetime on stress has been confirmed in tests lasting up to 18 months on a Kevlar rope of similar construction (see Reference [1], using data obtained from reference [8]).

Further tests on Parafil, lasting years rather than weeks are clearly desirable; the present test rig based on hydraulically applied loads would be unsuitable for these tests. However, even if the linear trend was found to continue at the lower stress levels, the problem of determining any degree of reliability or probability of failure would remain unless a very large number of tests were undertaken. Fortunately, a large number of tests on the core material of Parafil Type G ropes (Kevlar 49) has already been conducted [7]. Justification for use of the large database of results generated by this research, to overcome the reliability problem, is given in reference [4] thus obviating the need for conducting a large number of tests on full-scale ropes.

## 6. Conclusions

The conclusions are as follows.

(1) A thorough understanding of the long-term stress-rupture behaviour of Parafil Type G ropes is of prime importance if they are to prove viable alternatives to traditional materials for use as tendons in prestressed concrete.

(2) Extrapolation of lifetime data from short-term stress-rupture tests on 60 tonne ropes (lasting up to five months) indicates that a load equal to 50% of the nominal breaking load would cause failure after 100 years.

(3) Creep strains were observed to be dependent upon the creep load; an alternative method for

predicting long-term stress-rupture lifetimes based on strain data was thus postulated. Based on this method a load equal to 67% of the nominal breaking load was predicted to cause creep failure after 100 years. The predictions were found to be very dependent upon the assumed correlation between creep strain rate and stress. At present there is insufficient data to determine an accurate correlation, but work by others suggests that predictions based on direct extrapolation of lifetime data are likely to be more accurate.

(4) The limited number of tests conducted in this study have enabled general trends of stress-rupture behaviour to be established. For purposes of structural design, however, the need to attach a probability of failure to a material under stress is of paramount importance. A method for determining such probabilities for Parafil ropes utilizing the limited data from this research has consequently been developed and is discussed in reference [4].

### Acknowledgement

The work described here is part of an ongoing research programme in which structural applications of Parafil ropes are being investigated. The sponsors of this particular part of the programme were ICI Linear

Composites Ltd. and the Science and Engineering Research Council.

### References

1. J. J. CHAMBERS, PhD Thesis, University of London (1986).
2. ICI Linear Composites Ltd., trade literature.
3. G. B. GUIMARAES, Proceedings of Symposium on Engineering Applications of Parafil Ropes, edited by C. J. Burgoyne, Imperial College, January 1988 (Imperial College).
4. J. J. CHAMBERS and C. J. BURGOYNE, "Theoretical predictions of long-term stress-rupture behaviour of parallel-lay aramid ropes". In preparation.
5. M. H. HORN, P. G. RIEWALD and C. H. ZWEBEN, Proceedings of the Oceans 1977 Conference (Marine Tech. Soc. and I.E.E.E.), pp. 24E1-24E12.
6. A. HOWARD and N. J. PARRATT, Proceedings of the SAMPE Conference, San Diego, 1985 (Sampe).
7. R. E. GLASER, R. L. MOORE and T. T. CHIAO, *Compos. Technol. Rev.* 6 (1984) p. 26.
8. K. M. FERER, "Effects of long-term tension on Kevlar aramid fibre". Naval Ocean Research and Development Activity, National Space Technology Laboratories, Bay St Louis, Ms 39529, 1977.

*Received 24 February  
and accepted 30 August 1989*